

Dynamic criticality far-from-equilibrium: one-loop flow of Burgers-Kardar-Parisi-Zhang systems with broken Galilean invariance

Philipp Strack*

Institut für Theoretische Physik, Universität zu Köln, D-50937 Cologne, Germany and

Department of Physics, Harvard University, Cambridge MA 02138

(Dated: August 25, 2022)

Abstract

We study dissipative soft matter systems subject to random driving with long-range temporal correlations the latter purposefully breaking the Galilean invariance of Burgers-Kardar-Parisi-Zhang fluids and interfaces. We compute the phase diagram and critical exponents of the KPZ equation with $1/f$ -noise in spatial dimensions $1 \leq d < 4$ using the dynamic renormalization group with a frequency cutoff technique in a one-loop truncation. We find the rough phase at high noise levels to violate fluctuation-dissipation relations, to exhibit hyperthermal statistics and self-organized criticality, and thereby to constitute a universality class truly far removed from thermal equilibrium. The fixed point associated with the roughening transition fulfills an emergent thermal-like fluctuation-dissipation relation. We point out potential connections to nonlinear hydrodynamics with a reduced set of conservation laws and noisy quantum liquids.

*Electronic address: pstrack@physics.harvard.edu

Contents

I. Introduction	2
A. Key results	3
B. Organization of paper	8
II. Burgers-Kardar-Parisi-Zhang equation with $1/f$-noise	8
A. Broken Galilean invariance from $1/f$ -noise	9
B. Keldysh path integral representation	10
C. Mini-recap of known results without broken Galilean invariance	11
III. Dynamic renormalization group	12
A. Truncation and frequency cutoff technique	12
B. One-loop flow equations	14
IV. Solving the flow	17
A. Hyperthermal fixed point in the rough phase	17
B. Fixed point at the roughening transition	18
C. Numerical flows	19
V. Conclusions	21
Acknowledgments	21
A. Threshold functions	22
References	23

I. INTRODUCTION

A lot of effort across the physical sciences is currently being directed at the derivation of the laws of statistical mechanics far-from-(thermal)-equilibrium [1]. A prototypical question of interest begins with a many-particle system in a known initial state, whose statistics for example in energy space is known. Subsequently, the system is subjected to either a rapid change of its

parameters or a non-equilibrium drive and/or dissipation. One then would like to understand how the statistical distributions evolve in time, in particular with regard to thermalization properties, that is, how quickly and by which mechanisms, energy/momenta are redistributed in phase space and real space. The steady-state distributions in the long-time limit $t \rightarrow \infty$ are also interesting.

Roughly speaking, there are two extreme scenarios: (i) Integrable systems with a large number of conservation laws whose thermalization is at least slow due to constraints in phase space from these conservation laws (see Ref. 2 and references therein). (ii) Granular or soft matter systems such as hard spheres in a box, or randomly sputtered interfaces [3], in which the concept of temperature, a priori, does not make sense, there are typically few conserved quantities, and the dynamics is determined by geometric constraints, dimensionality, and/or the amount of disorder.

In order to elucidate the role of conservation laws in the dynamics of such soft matter systems, the present paper studies the phase structure and dynamics of Burgers-Kardar-Parisi-Zhang systems after *explicitly breaking its key symmetry: the Galilean invariance* of the randomly stirred Burgers fluid associated with seeing the same physics when looking at the fluid in a moving frame [4]. A particular focus of the present paper will be on what corresponds to the rough phase in interface context [5] or turbulent regimes in the fluid context [6–10]. An additional motivation is to build a framework and intuition for quantum matter out-of-equilibrium (Refs. 11–13 have recently asserted KPZ scaling in superfluids and quantum liquids).

A. Key results

Our calculations are based on the Cole-Hopf transformed KPZ equation (recapitulated below), when it becomes a gapless diffusion equation with multiplicative noise

$$\gamma \partial_t \phi = \nu_0 \nabla^2 \phi + \frac{\lambda}{2\nu} \phi \eta \quad (1)$$

with $\phi = \phi(t, \mathbf{x})$ a scalar field describing fluctuations in time and space around a growing average height level, γ a friction parameter, and ν_0 the viscosity in the Burgers fluid picture. The η -field acts as nonlinear, multiplicative noise [14] with coupling strength proportional to λ [15]. A simple way to break the Galilean invariance is to endow the noise with $1/f$ -correlations in time such that in frequency representation

$$\overline{\eta(\omega', \mathbf{x}') \eta(\omega, \mathbf{x})} = D_{1/f}(\omega) \delta(\omega + \omega') \delta^{(d)}(\mathbf{x}' - \mathbf{x}) . \quad (2)$$

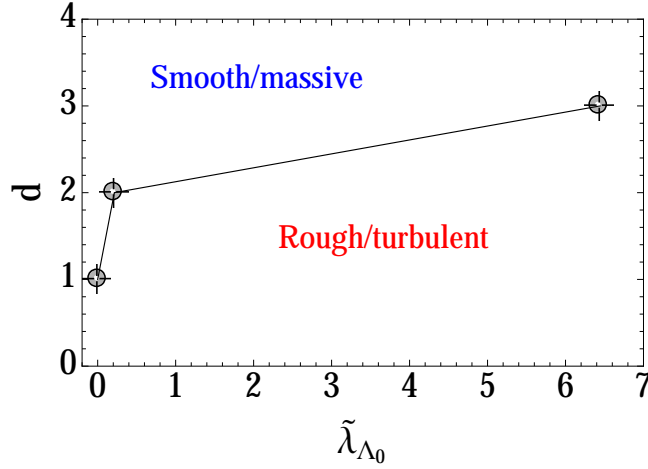


FIG. 1: Phase diagram of the KPZ equation with $1/f$ noise (computed points are connected as a guide to the eye) as a function of space dimensions (d) and strength of the bare noise vertex $\tilde{\lambda}_{\Lambda_0}$. The locators illustrate the roughening transition characterized by an unstable fixed point whose exponents fulfill an emergent thermal fluctuation-dissipation relation. In one dimension, the interface is always rough and any initial value of the noise vertex leads to the hyperthermal fixed point in the rough/turbulent phase. The other numerical parameters are: $\Lambda_0 = 10$, and the generated mass variable is always initially zero $\tilde{\Delta}_{\Lambda_0} = \Delta_{\Lambda_0} = 0$, because it is not present in the bare model Eq. (1).

with ubiquitous $1/f$ or pink noise temporal correlations [16]

$$D_{1/f}(\omega) = \frac{1}{|\omega|} . \quad (3)$$

Noise spectra with power-law correlations in momentum space have been applied to randomly stirred fluids [4], inertial-range and fully-developed turbulence [6, 9, 10], interface growth and directed polymer physics [15, 17]. Correlated noise of the form Eq. (2) was also investigated for an $O(N)$ -Ginzburg-Landau model [18]. In the context of turbulence, the noise derives from another stochastic process such as the elimination of fluid modes. Variants of Kolmogorov scaling in the velocity-velocity correlator can be obtained depending on the power-law exponent of the noise correlations [9]. As long as the noise is temporally white, however, the Galilean invariance is still preserved and the regime of interest in the present paper cannot be reached.

Fig. 1 shows the phase diagram obtained from a one-loop dynamic renormalization group analysis of Eq. (1) with $1/f$ -noise integrating fluctuations from large frequencies $\omega = \Lambda_0$ to the lowest frequencies $\omega = 0$. In spatial dimensionality $d = 2, d = 3$, a massive phase for small $\tilde{\lambda}_{\Lambda_0}$ transits

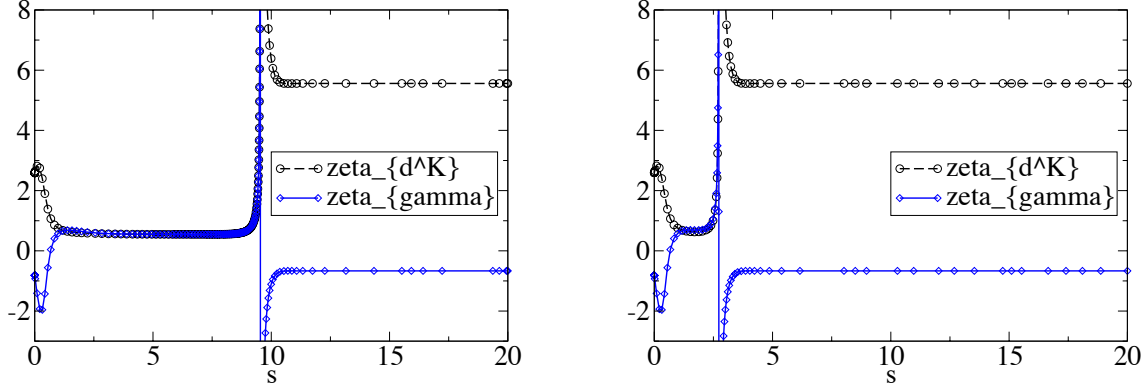


FIG. 2: Flow of the anomalous exponents slightly beyond the roughening transition in the rough phase in $d = 3$. The flow goes from the UV (left of plot) to IR (right of plot) via $\Lambda = \Lambda_0 \exp(-s)$. Left: $\tilde{\lambda}_{\Lambda_0} = 6.44294680824$, Right: $\tilde{\lambda}_{\Lambda_0} = 6.6443$, both larger than $\tilde{\lambda}_{\Lambda_{0,c}}$. The scaling plateaus of the roughening transition at which $\zeta_{d^K} = \zeta_\gamma = 0.54$ for $d = 3$ from Eq. (8) become unstable (at $s \approx 10$ in the left plot) and there is a steep transit into the rough phase, breaking the fluctuation-dissipation relation, at which $\zeta_{d^K} = 5.56$ and $\zeta_\gamma = -0.66$ from Table I in $d = 3$. Fine-tuned to 13 digits the critical noise vertex for the roughening transition is $\tilde{\lambda}_{\Lambda_{0,c}} = 6.4429468082319$ with $\Lambda_0 = 10$, $\Delta_{\Lambda_0} = \tilde{\Delta}_{\Lambda_0} = 0$ (no mass in the bare model Eq. (1)).

into a rough or turbulent phase at a critical value $\tilde{\lambda}_{\Lambda_{0,c}}$. A related phase diagram for the usual KPZ universality class preserving Galilean invariance can be found in Ref. [5], its detailed phase structure including long-range correlated noise in *space* was previously analyzed in Ref. 17.

The roughening transition and self-organized critical, rough phase are distinguishable by different scaling forms of the response correlator:

$$\mathcal{R}(\omega, \mathbf{k}) = -2\text{Im}\overline{\langle\phi(-\omega, -\mathbf{k})\phi(\omega, \mathbf{k})\rangle_R} \Rightarrow \mathcal{R}(s^z\omega, s\mathbf{k}) \propto \frac{1}{s^{2-\zeta_\gamma}} \mathcal{R} \quad (4)$$

and the independent Keldysh fluctuation correlator

$$C(\omega, \mathbf{k}) = i\overline{\langle\phi(-\omega, -\mathbf{k})\phi(\omega, \mathbf{k})\rangle_K} \Rightarrow C(s^z\omega, s\mathbf{k}) \propto \frac{1}{s^{4-2\zeta_\gamma+\zeta_{d^K}}} C, \quad (5)$$

where the overbar denotes the average over the random forces or noise. ζ_γ is the anomalous exponent for the linear time derivative in Eq. (1) and appears in the effective viscosity $\tilde{\nu} = \frac{\nu_0}{\gamma}$. ζ_{d^K} is the exponent for the effective noise spectrum, appearing in the statistical or Keldysh component defined below. A finite value of the exponent $\zeta_{\text{hyper}} = \zeta_{d^K} - \zeta_\gamma$ indicates deviations from thermal occupation of low-energy modes for which $\zeta_{\text{hyper}} = 0$. This can be seen from the scaling form of

	$d = 1$	$d=2$	$d=3$
ζ_{d^K}	15.68	8.30	5.56
ζ_γ	-6	-2	-2/3
ζ_{hyper}	21.68	10.30	6.23
z	8	4	2.66

TABLE I: One-loop values of critical exponents in the self-organized, rough phase. Explicit violation of a thermal fluctuation-dissipation relation is observed for which instead $\zeta_\gamma = \zeta_{d^K}$. The effective scale-dependent viscosity $\tilde{\nu}_\Lambda = \frac{\nu_0}{\gamma_\Lambda} \sim \Lambda^{\zeta_\gamma}$ diverges in entire the rough phase as $\zeta_\gamma < 0$.

the statistical distribution function

$$f(\omega, \mathbf{k}) = \frac{C(\omega, \mathbf{k})}{\mathcal{R}(\omega, \mathbf{k})} \Rightarrow f(s^z \omega, s\mathbf{k}) \Rightarrow \frac{1}{s^{2+(\zeta_{d^K}-\zeta_\gamma)}} \frac{C}{\mathcal{R}}. \quad (6)$$

For larger noise vertex $\tilde{\lambda}_{\Lambda_0} > \tilde{\lambda}_{\Lambda_0,c}$, in the rough or turbulent phase, the flow is attracted toward a gapless fixed point which breaks the fluctuation-dissipation relation of the KPZ equation with white noise [3, 19] as is shown in Fig. 2. The low-energy statistics in this phase is “hyperthermal”, that is the low-energy mode power-law divergence is stronger than thermal with $\zeta_{\text{hyper}} = 6.23$ in $d = 3$. Such infra-red enhanced population has been obtained at non-thermal fixed points of other field-theoretical models (see e.g. Refs. 7, 8 and references therein).

The response function exponent turns out to be negative in the rough phase

$$\zeta_\gamma = \frac{2(d-4)}{d} \quad (7)$$

and the full set of critical exponents in the rough phase are in Table I. The large value of the exponents in $d = 1, d = 2$ are due to the one-loop approximation and the fact the the noise vertex is relevant for $d < 4$. The one-loop computation is perturbatively controlled only close to $d = 4$.

The rough/turbulent phase is self-organized critical in the sense that it is does not require fine-tuning of the coupling constants to reach it. Rather, the *same* fixed point is reached for all $\tilde{\lambda}_{\Lambda_0} > \tilde{\lambda}_{\Lambda_0,c}$ as can be seen from flows of the mass parameter in Fig. 3. Note that the initial value

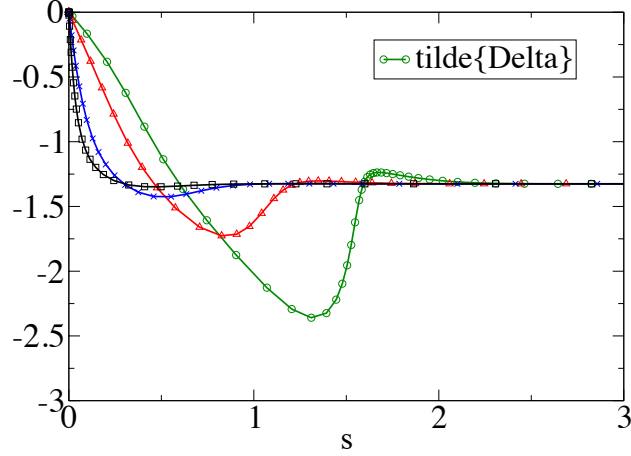


FIG. 3: Self-organized critical flows of the rescaled mass $\tilde{\Delta}_\Lambda$ in the rough phase in $d = 3$, which is attracted to the *same* fixed point value for different values of the noise vertex. $\tilde{\lambda}_{\Lambda_0} = 7, 10, 20, 30$ from green circles (7) to black squares (30). The initially zero mass (no mass in bare model Eq. (1)) is generated. The physical mass $\Delta_\Lambda = \tilde{\Delta}_\Lambda \Lambda^2 \gamma$ vanishes at the end of the flow for all couplings $\tilde{\lambda}_{\Lambda_0} \geq \tilde{\lambda}_{\Lambda_0,c}$. No fine-tuning of parameters required to reach this self-organized critical phase. The flow goes from the UV (left of plot) to IR (right of plot) via $\Lambda = \Lambda_0 \exp(-s)$.

of the mass Δ_{Λ_0} is always zero as appropriate for the gapless interface. Self-organized critical phases in open systems have of course been discussed in a variety of contexts (see e.g. Hwa and Kardar [20] for a one-loop analysis of sandpile models and Ref. 21 for a broader discussion on symmetries). Eq. (1) yields self-organized criticality with a relatively simple coupling to noise with a ubiquitous $1/f$ -spectrum [16]. Typically, as discussed in Ref. 21, the dissipative processes must be conditioned exquisitely in time. A further appealing feature of the simple model Eq. (1) with $1/f$ -noise is that the rough phase can be penetrated with the relatively simple one-loop RG.

At the roughening transition (rt) in $d = 2$ and $d = 3$, the asymptotically gapless dynamics fulfills an emergent thermal-like fluctuation-dissipation relation ($\zeta_{\text{hyper}} = 0$) with

$$\zeta_\gamma^{\text{rt}} = \zeta_{d^k}^{\text{rt}} = \frac{2d}{8+d} \quad \Rightarrow \quad z^{\text{rt}} = 2 - \zeta_\gamma^{\text{rt}} = \frac{16}{8+d} \quad (8)$$

where z is the dynamical exponent at one-loop. This scaling is also seen in the unstable scaling plateaus of Fig. 2 and further numerical flows are presented in the main text. At the roughening transition, the effective viscosity $\tilde{\nu}_\Lambda = \frac{\nu_0}{\gamma_\Lambda} \sim \Lambda^{\zeta_\gamma}$ vanishes as $\zeta_\gamma^{\text{rt}} > 0$ at one-loop. This is in contrast to the rough phase where the effective viscosity diverges as $\zeta_\gamma < 0$ from Table I.

B. Organization of paper

In Sec. II, we recapitulate the relations between the Burgers, KPZ, and diffusion equation with multiplicative noise. Following Medina, Hwa, Kardar, and Zhang (MHKZ) [15], we show how temporal correlations in the noise break the Galilean invariance of the Burgers fluid. Then, we elevate the equation to an action on the closed-time Keldysh action in Subsec. II B. In Subsec. II C, we briefly survey simplifications arising from the Galilean invariance such as exponent identities and a fluctuation-dissipation relation.

In Sec. III, we present the dynamic RG framework, explain the frequency cutoff technique and derive the form of the flow equations to one-loop order.

In Sec. IV, we present analytical and numerical solutions to the flow equations.

In Sec. V, we offer some conclusions, point toward physical systems where our results may become relevant for, and outline potential directions for future work.

II. BURGERS-KARDAR-PARISI-ZHANG EQUATION WITH $1/f$ -NOISE

According to Kardar, Parisi, and Zhang [3], coarse-grained fluctuations in the growth of a d -dimensional interface subject to random depositions can be described in terms of a scalar height function

$$\frac{\partial h}{\partial t} = \nu_0 \nabla^2 h + \frac{\lambda}{2} (\nabla h)^2 + \eta, \quad (9)$$

where both the height $h = h(t, \mathbf{x})$ and the noise $\eta = \eta(t, \mathbf{x})$ are functions of time t and d -dimensional interface space spanned by \mathbf{x} .

Upon identifying the height with a vorticity-free velocity field $\mathbf{v} = -\nabla h$ and the random deposition noise with a random stirring force $\mathbf{f} = -\nabla \eta$, Eq. (9) is equivalent to the Burgers equation

$$\partial_t \mathbf{v} + \lambda \mathbf{v} \cdot \nabla \mathbf{v} = \nu_0 \nabla^2 \mathbf{v} + \mathbf{f}, \quad (10)$$

where ν_0 is the fluid viscosity, and the coefficient λ parametrizes the relative strength of the non-linear, convective term [6]. In this paper, we will work with the representation of Eq. (9) as a diffusion equation for $\phi(t, \mathbf{x}) = \exp [(\lambda/2\nu_0)h(t, \mathbf{x})]$ given above in Eq. (1) supplemented by the friction constant γ .

A. Broken Galilean invariance from $1/f$ -noise

The form of the noise correlator $\overline{\eta(t', \mathbf{x}')\eta(t, \mathbf{x})}$ in Eq. (3) determines the physical context and shapes the solution space of Eqs. (1,9,10). The question of what happens to interface fluctuations/stirred fluids subject to such temporally correlated noise was raised, but not conclusively answered by MHKZ [15]. The reason why this case is qualitatively different is that the temporal correlations in the noise break the Galilean invariance of the Burgers equation (10) under

$$\mathbf{v}(t, \mathbf{x}) \rightarrow \mathbf{v}_0 + \mathbf{v}'(\mathbf{x} - \lambda \mathbf{v}_0 t, t) \quad (11)$$

associated with looking at the fluid in a moving frame [4, 15]. To be self-contained, we now recapitulate why this is so following App. B of Ref. 15. For the interface equation (9) the Galilean invariance translates into invariance under infinitesimal tilts by a small angle ϵ

$$\begin{aligned} h' &= h + \epsilon \cdot \mathbf{x} \\ \mathbf{x}' &= \mathbf{x} + \lambda \epsilon t' \\ t' &= t \end{aligned} \quad (12)$$

It is easy to see that the deterministic part of Eq. (9) is invariant under Eq. (12). It is also invariant under constant height shifts $h \rightarrow h + \text{const}$ due to the absence of mass term or pinning potential. The transformed equation for h' is subject to transformed noise $\eta'(t', \mathbf{x}') = \eta(t', \mathbf{x} + \lambda \epsilon t')$ implying for the noise correlator

$$\begin{aligned} F' &= \overline{\eta'(t'_1, \mathbf{x}'_1)\eta'(t'_2, \mathbf{x}'_2)} = \overline{\eta(t_1, \mathbf{x}_1 + \lambda \epsilon t_1)\eta(t_2, \mathbf{x}_2 + \lambda \epsilon t_2)} \\ &= F(t_1 - t_2, \mathbf{x}_1 - \mathbf{x}_2 + \lambda \epsilon(t_1 - t_2)) \\ &= \delta(t_1 - t_2)F(\mathbf{x}_1 - \mathbf{x}_2 + \lambda \epsilon(t_1 - t_2)) = \delta(t_1 - t_2)F(\mathbf{x}_1 - \mathbf{x}_2) = F \end{aligned} \quad (13)$$

where the last line is only if true the noise has no correlations in time i. e. $F(t, \mathbf{x}) = \delta(t)F(\mathbf{x})$.

Our choice Eq. (3) corresponds to power-law correlations in real time and violates the invariance Eq. (13), as announced in the Introduction. Despite the naturalness of considering ubiquitous $1/f$ noise and its potential connections to a critical continuum of fluid modes in turbulent flows, this case was not considered by MHKZ [15], apparently due to the technical difficulty of dealing with a noise spectrum that is infrared singular in frequency space and the necessity to perform the scaling procedure on frequencies rather than on momenta.

B. Keldysh path integral representation

In order to explore the large distance and long time physics of the Burgers-Kardar-Parisi-Zhang systems subject to $1/f$ -noise, we elevate the stochastic differential equation problem Eq. (1) plus Eq. (3) to a Keldysh path integral on the closed time contour [22, 23]. Wherever possible, we will follow the notation of Frey and Täuber [19], who reviewed and performed this procedure and have given Ward and exponent identities for the related Janssen-De Dominicis functional.

The random forces are taken to be Gaussian-distributed

$$W[\eta] \propto \exp \left\{ - \int d^d x \int d\omega \frac{1}{2} \eta(\omega, \mathbf{x}) |\omega| \eta(\omega, \mathbf{x}) \right\}. \quad (14)$$

Then, the fluctuations in η can be included on the same footing as the fluctuations of ϕ in the Keldysh generating functional

$$\begin{aligned} Z &= \int \mathcal{D}\eta W[\eta] \mathcal{D}(\phi, \tilde{\phi}) e^{i(S_\phi[\phi, \tilde{\phi}] - \int_{t,x} \eta \phi \tilde{\phi})} \\ &\equiv \int \mathcal{D}(\eta, \phi, \tilde{\phi}) e^{i(S_\phi[\phi, \tilde{\phi}] + S_\eta[\eta] + S_\lambda[\phi, \tilde{\phi}, \eta])}. \end{aligned} \quad (15)$$

The momentum-independent noise propagator is now complex-valued

$$S_\eta[\eta] = \frac{1}{2} \int_{\omega, \mathbf{q}} \eta(-\omega, -\mathbf{q}) [G^\eta(\omega)]^{-1} \eta(\omega, \mathbf{q}). \quad (16)$$

with

$$G^\eta(\omega) = \frac{-i}{|\omega|}. \quad (17)$$

Note that the momentum integrations here is bounded in the UV by some short-distance cutoff by virtue of a necessary smallest physical distance below which the noise is spatially uncorrelated and the continuum description must be replaced by a discrete theory of lattice sites/grains.

The multiplicative noise term in Eq. (1) results in a trilinear noise vertex

$$S_\lambda[\phi, \tilde{\phi}, \eta] = - \int_t dt \int d^d x \frac{\lambda}{2\nu_0} \eta(t, \mathbf{x}) \tilde{\phi}(t, \mathbf{x}) \phi(t, \mathbf{x}) \quad (18)$$

Finally, the dynamics, diffusion, and statistics (Keldysh $\tilde{\phi}\phi$ -component) of the ϕ -fields are comprised in a matrix propagator

$$S_\phi[\phi, \tilde{\phi}] = \frac{1}{2} \int d\omega \int d^d k (\phi \tilde{\phi}) \begin{pmatrix} 0 & [G^A(\omega, \mathbf{k})]^{-1} \\ [G^R(\omega, \mathbf{k})]^{-1} & D^K \end{pmatrix} \begin{pmatrix} \phi \\ \tilde{\phi} \end{pmatrix} \quad (19)$$

with the bare retarded and advanced Greens function given by

$$\begin{aligned} G^R(\omega, \mathbf{k}) &= \frac{1}{i\gamma\omega - \nu_0 \mathbf{k}^2} , \\ G^A(\omega, \mathbf{k}) &= \frac{1}{-i\gamma\omega - \nu_0 \mathbf{k}^2} , \end{aligned} \tag{20}$$

The statistical Keldysh component D^K contains the effective noise spectrum and will later be determined by loop corrections. Note that in absence of the initially zero D^K , the *bare* action Eq. (18) consists only of power of $\tilde{\phi}\phi$, which can also be traced to a kind of gauge transformation related to Galilean invariance [17]. The bare action still describes a gapless interface and is invariant under constant shifts of $\phi \rightarrow \phi + \text{const}$. As we discussed, without Galilean invariance, the action is not protected against mass generation and we will allow for such terms to be generated in the renormalization group (RG) flow below in Sec. III.

C. Mini-recap of known results without broken Galilean invariance

We here briefly recollect some previous results of the Burgers-KPZ field theories focussing in particular on the simplifications due to Galilean invariance in the case of temporally white noise. In spatial dimension $d < 2$ KPZ interfaces are always rough for any value of the nonlinearity λ , see e.g.: Ref. 5. For $d > 2$, a smooth phase is stable for small λ and there is a line of non-equilibrium roughening transitions separating the two. An important consequence of the ability to phrase the KPZ problem in one dimension as an "equilibrium" partition function of an elastic string in a random potential [3, 24] are fluctuation-dissipation relations [25] and Ward identities [19]. In particular, these insure that (i) the noise vertex λ is not renormalized at all orders in perturbation theory, (ii) the fluctuation spectrum D scales similarly to the dissipative viscosity $D/\nu_0 \rightarrow \text{const}$, and (iii) that the roughness exponent χ and dynamical exponent z fulfill the exact relation $\chi + z = 2$ with $z = 3/2$ [3, 15]. In absence of Galilean invariance, (i) - (iii) do not hold anymore. In particular also the continuous shift invariance $h \rightarrow h + \text{const}$ can now be violated by loop corrections.

To explore the interface dynamics constrained by only a reduced set conserved quantities (essentially only momentum and parity), we next perform a dynamic renormalization group analysis.

III. DYNAMIC RENORMALIZATION GROUP

We will compute the one-loop RG flow of the action Eq. (15) employing a frequency cutoff, that is, rescaling frequencies and integrating over all momenta at each RG step. Our analysis will be framed in the context of the flow equation for the effective Keldysh action $\Gamma_\Lambda[\phi, \eta]$ as a function of a continuous flow parameter Λ (see Refs. 26, 27 for condensed matter applications):

$$\partial_\Lambda \Gamma_\Lambda[\phi, \eta] = \frac{i}{2} \text{Tr} \left[\frac{\dot{\mathcal{R}}}{\Gamma_\Lambda^{(2)}[\phi, \eta] + \mathcal{R}} \right], \quad (21)$$

where the trace stands for a frequency and momentum integration and a simple matrix trace in field space over the c and q components, and the noise field η , respectively. \mathcal{R} is a matrix containing cutoff functions (specified below) as convenient for the field basis (ϕ_c, ϕ_q, η) :

$$\mathcal{R} = \begin{pmatrix} 0 & R_\Lambda^\phi & 0 \\ R_\Lambda^\phi & 0 & 0 \\ 0 & 0 & R_\Lambda^\eta \end{pmatrix}$$

$\Gamma^{(2)}$ is a matrix containing the second field derivatives of Γ evaluated at zero field whose inverse contains the scale-dependent Green's functions that we define below.

A. Truncation and frequency cutoff technique

We now specify which parameters we keep out of the formally large set of coupling constants that can be generated under the RG flow. In particular, it will be important to introduce independent parameters for the response function and the Keldysh spectrum. That allows the flow to break equilibrium-like fluctuation-dissipation relations. We also introduce a mass term. Note that ϕ , $\tilde{\phi}$ and η all have bare scaling dimension $\left[\frac{d}{2}\right]$ under bare $\omega \sim \Lambda^2$ power counting. This makes the trilinear noise vertex λ_Λ formally relevant in $d < 4$. Therefore, our truncation should be under sound control if $\epsilon = 4 - d$ is small.

Propagator renormalizations are captured by introducing four flowing parameters γ_Λ , A_Λ , a mass term Δ_Λ , and d_Λ^K for the (independent) Keldysh component. Together with the noise vertex, this is also the minimal set of couplings that one would have to renormalize for example within a field-theoretic RG analysis [19]. Including the additive, scale-dependent cutoff function R_Λ into

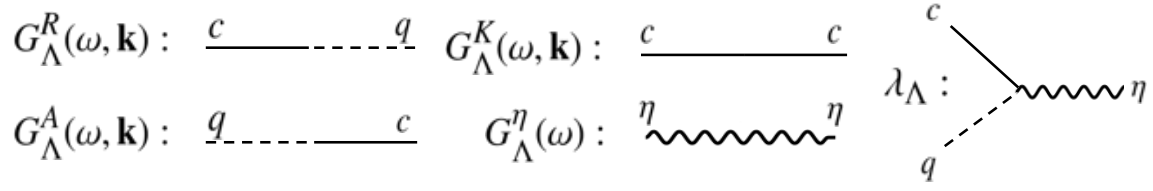


FIG. 4: Propagators and vertices appearing in the Keldysh action.

Eq. (19) the quadratic part of the flowing action is

$$\Gamma_{\Lambda}^{(2)\phi} = \frac{1}{2} \int_k (\phi \tilde{\phi}) \begin{pmatrix} 0 & [G_{\Lambda}^A(\omega, \mathbf{k})]^{-1} \\ [G_{\Lambda}^R(\omega, \mathbf{k})]^{-1} & D_{\Lambda}^K(\omega) \end{pmatrix} \begin{pmatrix} \phi \\ \tilde{\phi} \end{pmatrix} \quad (22)$$

with the now scale-dependent, retarded and advanced propagators

$$\begin{aligned} G_{\Lambda}^R(\omega, \mathbf{k}) &= \frac{1}{i\gamma_{\Lambda}\omega - (A_{\Lambda}\mathbf{k}^2 + \Delta_{\Lambda}) + R_{\Lambda}^R(\omega)} , \\ G_{\Lambda}^A(\omega, \mathbf{k}) &= \frac{1}{-i\gamma_{\Lambda}\omega - (A_{\Lambda}\mathbf{k}^2 + \Delta_{\Lambda}) + R_{\Lambda}^A(\omega)} , \end{aligned} \quad (23)$$

where the frequency cutoffs are complex conjugates of one another $R_{\Lambda}^A(\omega) = [R_{\Lambda}^R(\omega)]^*$. In contrast to the problem with full Galilean invariance, we will see that here a mass term is generated at one loop – we capture this flow by introducing Δ_{Λ} .

The Keldysh propagator $G^K = -G^R D^K G^A$ with $D_{\Lambda}^K(\omega) = 2id_{\Lambda}^K$ is

$$G_{\Lambda}^K(\omega, \mathbf{k}) = \frac{-2id_{\Lambda}^K}{[i\gamma_{\Lambda}\omega - (A_{\Lambda}\mathbf{k}^2 + \Delta_{\Lambda}) + R_{\Lambda}^R(\omega)]^2} . \quad (24)$$

At one-loop, the momentum coefficient does not flow and it remains fixed at its initial value $A_{\Lambda} = \nu_0$ from Eq. (1).

The flowing trilinear noise vertex

$$\Gamma_{\Lambda}^{(3)} = - \int_{t,x} \lambda_{\Lambda} \eta \tilde{\phi} \phi \quad (25)$$

is related to the bare vertex Eq. (18) at the beginning of the flow via $\lambda_{\Lambda=\Lambda_0} = \frac{\lambda}{2\nu_0}$.

The quadratic noise part in the action

$$\Gamma_{\Lambda}^{(2)\eta} = \frac{1}{2} \int_k \eta [G_{\Lambda}^{\eta}(\omega)]^{-1} \eta \quad (26)$$

is not renormalized and the inverse propagator needs only be supplemented by the cutoff

$$G_{\Lambda}^{\eta}(\omega) = \frac{-i}{|\omega| + R_{\Lambda}^{\eta}(\omega)} . \quad (27)$$

By endowing the noise propagator with a cutoff, the noise average is performed continuously along Λ , which may be viewed as flowing from the short time dynamics at large Λ to the long time dynamics at $\Lambda \rightarrow 0$. The Feynman graph elements of the flowing action are shown in Fig. 4.

As announced above, we will use frequency regulators with Eq. (21), which in Wilsonian RG language corresponds to rescaling frequencies and integrating over all momenta at each RG step.

The specific form of the frequency regulator for the noise field is

$$\begin{aligned} R_\Lambda^\eta(\omega) &= (-|\omega| + \Lambda^2) \theta[\Lambda^2 - |\omega|] \\ \partial_\Lambda R_\Lambda^\eta(\omega) &= 2\Lambda \theta(\Lambda^2 - |\omega|) , \end{aligned} \quad (28)$$

and for the ϕ -field we have

$$\begin{aligned} R_\Lambda^R(\omega) &= \gamma(-i\omega + i\text{sgn}(\omega)\Lambda^2) \theta[\Lambda^2 - |\omega|] \\ \dot{R}_\Lambda^R(\omega) \equiv \partial_\Lambda R_\Lambda^R(\omega) &= 2\Lambda i\gamma \text{sgn}(\omega) \theta[\Lambda^2 - |\omega|] \end{aligned} \quad (29)$$

and for its advanced complex conjugate

$$\begin{aligned} R_\Lambda^A(\omega) &= \gamma(+i\omega - i\text{sgn}(\omega)\Lambda^2) \theta[\Lambda^2 - |\omega|] \\ \dot{R}_\Lambda^A(\omega) \equiv \partial_\Lambda R_\Lambda^A(\omega) &= -2\Lambda i\gamma \text{sgn}(\omega) \theta[\Lambda^2 - |\omega|] . \end{aligned} \quad (30)$$

We also dropped, as usual, the higher-order scale derivatives $\partial_\Lambda \gamma$ in these expressions. Hard (e.g. [28]) and soft (e.g. [29]) frequency cutoffs are frequently also being applied in RG studies of strongly correlated fermionic systems.

B. One-loop flow equations

We now write down the explicit form of the flow equations following from expanding the master flow equation, Eq. (21), with the truncation specified above. For brevity, we will use an integration symbol that includes the cutoff derivatives:

$$\int = \int \frac{d^d \mathbf{k}}{(2\pi)^d} \int \frac{d\omega}{2\pi} [\dot{R}_\eta \partial_{R_\eta} + \dot{R}_\Lambda^R \partial_{R_\Lambda^R} + \dot{R}_\Lambda^A \partial_{R_\Lambda^A} .] \quad (31)$$

We get the expressions:

$$\begin{aligned} \partial_\Lambda (id_\Lambda^K) &= \frac{-i}{2} \int \lambda_\Lambda^2 G_\Lambda^\eta(\omega) G_\Lambda^K(\omega, \mathbf{k}) \\ \partial_\Lambda (-\Delta_\Lambda) &= \frac{-i}{2} \int \lambda_\Lambda^2 G_\Lambda^\eta(\omega) (G_\Lambda^A(\omega, \mathbf{k}) + G_\Lambda^R(\omega, \mathbf{k})) \\ \partial_\Lambda (-\lambda_\Lambda) &= \frac{-i}{2} \int \lambda_\Lambda^3 G_\Lambda^\eta(\omega) (G_\Lambda^A(\omega, \mathbf{k})^2 + G_\Lambda^R(\omega, \mathbf{k})^2) . \end{aligned} \quad (32)$$

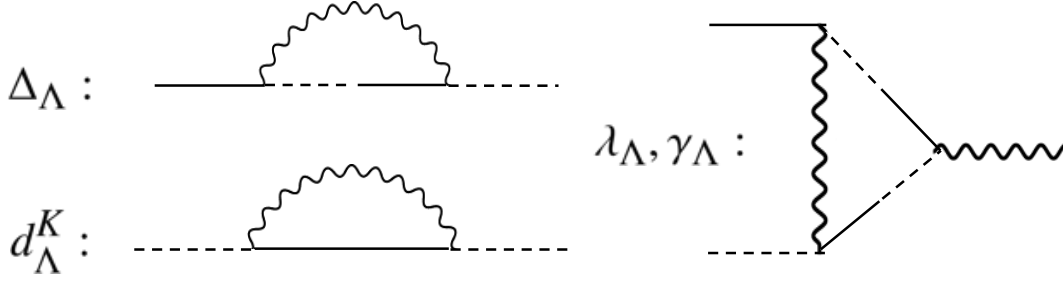


FIG. 5: One-loop contractions for Eq. (32). As for the flow of γ_Λ , the frequency derivative of the self-energy diagram for the retarded/advanced component (top left), generates the identical contraction as that for the noise vertex (right). This cancellation seems to be one reason for the self-organized nature of the rough phase as alluded to in the Introduction and observed in the numerics in Fig. 3.

The corresponding Feynman contractions are shown in Fig. 5. At the one-loop level, there is no flow for the momentum renormalization factor $\partial_\Lambda A = 0$ and the flow of the frequency renormalization factor γ_Λ is obtained via the diagrammatic identity

$$\zeta_\gamma = -\frac{\Lambda}{\gamma_\Lambda} \partial_\Lambda \gamma_\Lambda = -\frac{\Lambda}{\lambda_\Lambda} \partial_\Lambda \lambda_\Lambda = \zeta_\lambda. \quad (33)$$

More severe diagrammatic redundancies appear in gauge theories (for example QED or the CP^N -model), there as a consequence of truly conserved global charges [30, 31]. Here, the cancellation is probably a leftover effect of the expansion of the action in powers of $\tilde{\phi}\phi$, which can be traced back to a gauge transformation related to the Galilean invariance for temporally white noise [17].

The frequency integrations in Eqs. (32) become simple due the cutoff choice and for the rotationally symmetric momentum integrations it is convenient to use a rescaled momentum variable $\tilde{\mathbf{k}}^2 = \frac{A}{\gamma} \frac{\mathbf{k}^2}{\Lambda^2}$ such that the momentum integration measure becomes

$$d^d \mathbf{k} \rightarrow d^d \tilde{\mathbf{k}} \Lambda^d \left(\frac{\gamma}{A} \right)^{d/2}. \quad (34)$$

As announced above, we expect the continuum description to be valid only up to a short-distance of UV-momentum cutoff, below which the the granular/lattice structure of the interface becomes important. In order to regulate physically unimportant UV-divergences in the momentum integrations we systematically include only "on-shell" and smaller momenta into the flow

$$\mathbf{k}^2 \leq \frac{\gamma}{A} \Lambda^2, \quad \tilde{\mathbf{k}}^2 \leq 1. \quad (35)$$

As $\Lambda \rightarrow 0$, this is a shrinking ball around the origin in momentum space, whose volume is continuously adapted as γ flows, too. This mimicks the UV behavior from a Litim-type cutoff in

momentum space, which regulates both, IR and UV divergences [32]. We have checked that the findings and fixed points reported below do not qualitatively seem to depend on the regularization procedure and choice of cutoffs. We have repeated the calculation for a different cutoff and different UV regularization procedure and found similar results.

In addition to the anomalous exponents in Eq. (33), we define the rescaled variables for the mass variable and the noise vertex

$$\begin{aligned}\tilde{\Delta} &= \frac{\Delta_\Lambda}{\gamma_\Lambda \Lambda^2} \\ \tilde{\lambda} &= \frac{\lambda_\Lambda}{\Lambda^{(4-d)/2} A_\Lambda^{d/4} \gamma_\Lambda^{1-d/4} \sqrt{\pi}}\end{aligned}\tag{36}$$

and the slope of the statistical Keldysh component

$$\zeta_{d^K} = -\frac{\Lambda}{d_\Lambda^K} \partial_\Lambda d_\Lambda^K .\tag{37}$$

For completeness, we will write out the analogous exponent for the momentum factor $\zeta_A = -\frac{\Lambda}{A_\Lambda} \partial_\Lambda A_\Lambda$ in the equations below, but it vanishes at the one-loop level.

The various β -functions following from explicit evaluation of Eqs. (32) take on the simple form:

$$\begin{aligned}\Lambda \partial_\Lambda \tilde{\Delta} &= (-2 + \zeta_\gamma) \tilde{\Delta} + \tilde{\lambda}^2 D_{\lambda^2}[\tilde{\Delta}] \\ \Lambda \partial_\Lambda \tilde{\lambda} &= \left(\frac{d-4}{2} + \frac{d}{4} \zeta_A + \left(1 - \frac{d}{4}\right) \zeta_\gamma - \zeta_\lambda \right) \tilde{\lambda}\end{aligned}\tag{38}$$

together with the anomalous exponents

$$\begin{aligned}\zeta_A &= 0 \\ \zeta_{d^K} &= \tilde{\lambda}^2 S_{\lambda^2}[\tilde{\Delta}] \\ \zeta_\gamma &= \tilde{\lambda}^2 G_{\lambda^3}[\tilde{\Delta}] = \zeta_\lambda .\end{aligned}\tag{39}$$

Invoking $\zeta_A = 0$ and the identity $\zeta_\gamma = \zeta_\lambda$ the flow equation for the noise vertex simplifies to

$$\Lambda \partial_\Lambda \tilde{\lambda} = \left(\frac{d-4}{2} - \frac{d}{4} \zeta_\gamma \right) \tilde{\lambda} .\tag{40}$$

Partial cancellations in β -functions can be a reason for the appearance of anomalous exponents that depend only on dimensionality [20] and sometimes critical phases rather than critical points.

The fixed point structure is determined by dimensionality d and the properties of the three threshold functions $D_{\lambda^2}[\tilde{\Delta}]$, $S_{\lambda^2}[\tilde{\Delta}]$, and $G_{\lambda^3}[\tilde{\Delta}]$, which depend on the mass variable $\tilde{\Delta}$ and dimensionality $d = 1, 2, 3$. The analytic expressions and various limiting cases for the threshold functions are given in Appendix A.

IV. SOLVING THE FLOW

In this section, we solve the flow equations (38,39) first analytically in two limit cases complementary to the numerical solutions exhibited in the key results section I A. The initial value for the mass variable is zero $\Delta_{\Lambda_0} = 0$, having in mind a gapless interface before turning on the coupling to the noise. We will vary strength of the noise vertex λ_Λ to tune through the phase diagram shown Sec. I A from the massive phase (small initial $\tilde{\lambda}_{\Lambda_0}$) to the rough, but gapless phase (large $\tilde{\lambda}_{\Lambda_0}$) via critical point to the rough phase at $\tilde{\lambda}_{\Lambda_0,c}$. For $d > 1$, the critical point at the roughening transition is characterized by an unstable fixed point that fulfills an emergent fluctuation-dissipation relation, while the rough phase manifestly breaks this relation and the response function and the Keldysh spectrum scale with different exponents. In $d = 1$, the interface is always rough.

A. Hyperthermal fixed point in the rough phase

In $d < 4$, Eqs. (39,40) admit a stable non-Gaussian fixed point ($\Lambda \partial_\Lambda \tilde{\lambda} = 0$) solution

$$\begin{aligned}\zeta_\gamma &= \frac{2(d-4)}{d} \\ \tilde{\lambda}_*^2 &= \frac{2(d-4)}{d G_{\lambda^3}[\tilde{\Delta}_*]}\end{aligned}\tag{41}$$

provided the equation for the mass ($\Lambda \partial_\Lambda \tilde{\Delta} = 0$) has a solution

$$\tilde{\Delta}_* = \frac{d-4}{4} \frac{D_{\lambda^2}[\tilde{\Delta}_*]}{G_{\lambda^3}[\tilde{\Delta}_*]}\tag{42}$$

such that $\tilde{\lambda}_*^2 > 0$ with $\tilde{\lambda}$ a real-valued number. This is indeed the case in $d = 1, 2, 3$ as is shown in Fig. 6 for $d = 2$. Of course, a fixed point $\tilde{\Delta}^*$ means that the physical mass vanishes during the flow

$$\Delta = \tilde{\Delta}^* \Lambda^2 \gamma \xrightarrow{\Lambda \rightarrow 0} 0\tag{43}$$

implying that the entire rough phase is gapless. This fixed point is accompanied by a set of critical exponents including the dynamical exponent

$$z = 2 + \zeta_A - \zeta_\gamma = 2 - \zeta_\gamma\tag{44}$$

collected in Table I. In the rough phase, the strong-coupling between the "flat $z = \infty$ spectrum" (local in space) of the noise propagator and the bare $z = 2$ overdamped ϕ -dynamics leads to z -values intermediating between the two values. Note that the steep flow when the scaling of the roughening transition changes to that of the rough phase in Fig. 2, is due to a change of sign of the threshold function for ζ_γ . This function, $G_{\lambda^3}[\tilde{\Delta}]$, is plotted in the Appendix A.

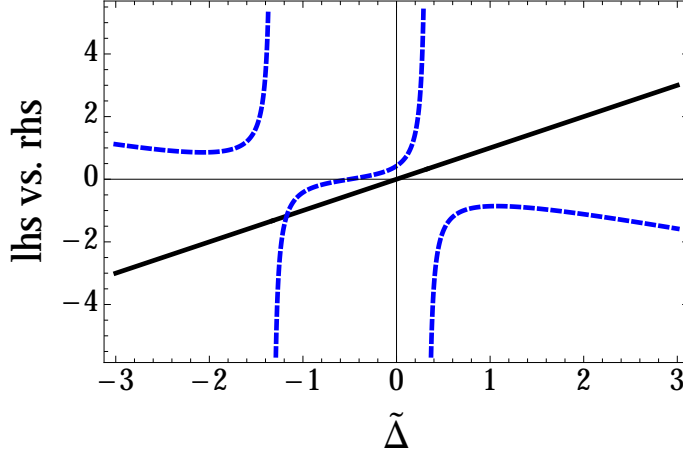


FIG. 6: Fixed point for $\tilde{\Delta}^* = -1.174$ in the rough phase in $d = 2$ from finding intersections of the left-hand-side of Eq. (42) (black line) with its right-hand-side (blue, dashed line). As at the Wilson-Fisher fixed point for the $O(n)$ model [33], the rough phase fixed point, $(\tilde{\Delta}^* = -1.396, \tilde{\lambda}^* = 10.154)$ also in $d = 3$, lies at negative mass in the plane of rescaled mass vs. rescaled coupling. This is true in all dimensions $d = 1, 2, 3$.

B. Fixed point at the roughening transition

The fixed point at the roughening transition (rt) is analyzed in changed variables

$$\begin{aligned}\tilde{\Delta}_{\text{rt}} &= \tilde{\Delta} \Lambda^2 \gamma^2 \\ \tilde{\lambda}_{\text{rt}} &= \tilde{\lambda} \Lambda^2 \gamma^2\end{aligned}\tag{45}$$

which attain fixed points at the roughening transition, $(\tilde{\Delta}_{\text{rt}}^* = -5.81, \tilde{\lambda}_{\text{rt}}^* = 23.33)$ in $d = 3$, whose ratio turns out to be fixed to be $\left| \frac{\tilde{\lambda}_{\text{rt}}^*}{\tilde{\Delta}_{\text{rt}}^*} \right| = 3\pi \sqrt{\frac{2}{11}}$. This leads to an automatic fulfillment of the vanishing of the β -function indicative of an asymptotically unstable fixed point. In the numerics, this is reflected by shorter and somewhat more wobbly scaling plateaus of the mass and vertex when compared to the stable fixed point of the rough phase.

This means that the physical mass vanishes $\Delta_\Lambda = \tilde{\Delta}_{\text{rt}}/\gamma \sim \Lambda^{\zeta_\gamma^{\text{rt}}}$ as can be seen in Fig. 7.

$$\partial_t \tilde{\lambda}_{\text{rt}} = \left(\frac{d}{2} - \left(1 + \frac{d}{4}\right) \zeta_{\gamma_{\text{rt}}} - \zeta_{\lambda_{\text{rt}}} \right) \tilde{\lambda}_{\text{rt}}\tag{46}$$

implying (with $\zeta_{\gamma_{\text{rt}}} = \zeta_{\lambda_{\text{rt}}}$) Eq. (8). The emergent thermal fluctuation-dissipation relation is easily seen as follows. When $\tilde{\Delta}_{\text{rt}}^*$ attains a constant fixed point value, the “old” variable $\tilde{\Delta}$ must diverge. Expanding the threshold functions in Appendix A for the Keldysh component (in “old” variables

and for concreteness in $d = 3$)

$$\zeta_{d^k} = \tilde{\lambda}^2 S_{\tilde{\lambda}^2}[\tilde{\Delta}] \xrightarrow{\tilde{\Delta} \rightarrow \infty} \approx \tilde{\lambda}^2 \frac{1}{3\pi^2 \tilde{\Delta}^2} = \tilde{\lambda}^2 G_{\lambda^3}[\tilde{\Delta} \rightarrow \infty] = \zeta_\gamma. \quad (47)$$

Note that the ratio $\frac{\tilde{\lambda}^2}{\tilde{\Delta}^2}$ is invariant under the variable change Eq. (45) and consequently $\zeta_\gamma^{\text{rt}} = \zeta_{d^k}^{\text{rt}}$ as seen in the explicit flows in Subsec. I A and Subsec. IV C.

C. Numerical flows

We briefly describe the numerical procedure and initial conditions for the explicit flows in Subsec. I A. We also show a few of more plots: Fig. 7,8 for flows in the massive phase upon approaching the roughening transition and Fig. 9 as exemplary flow deep in the rough phase. The coupled flow equations (38,39) are integrated using a fourth order Runge Kutta routine (results did not change from using different routines) from high frequencies $\Lambda_0 = 10$ down to $\Lambda = 0$ using the momentum-integrated version of the threshold functions given in the Appendix A. We always begin the flow with zero initial mass $\Delta_{\Lambda_0} = \tilde{\Delta}_0$ as appropriate for the gapless interface. The initial

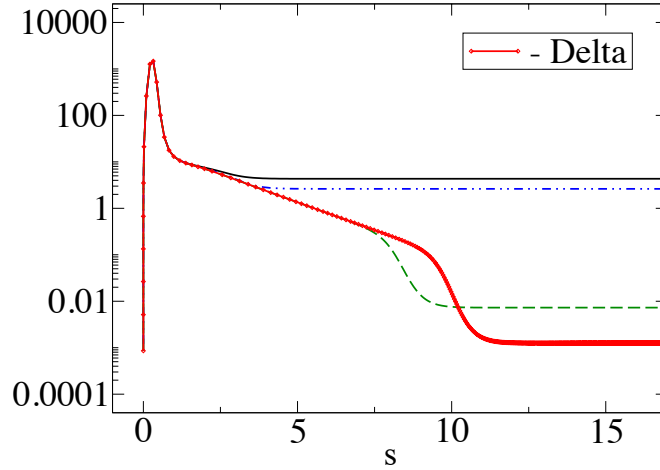


FIG. 7: Flow of the physical (non-rescaled) mass $-\Delta_\Lambda$ in $d = 3$ upon approaching the roughening transition from the massive phase in double logarithmic graph. The mass is initially numerically zero $\Delta_{s=0} = 0$. The red line is closest to $\tilde{\lambda}_{\Lambda_0,c}$ from below. For infinite numerical accuracy the power-law linear scaling with slope $\zeta_\gamma^{\text{rt}} = 6/11 = 0.54$ from Eq. (8) for the roughening transition would extend longer and longer. The flow goes from the UV (left of plot) to IR (right of plot) via $\Lambda = \Lambda_0 \exp(-s)$.

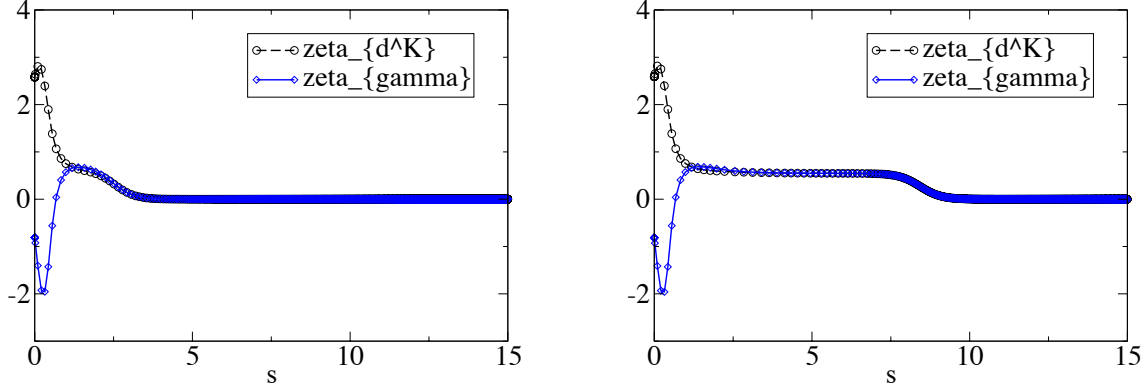


FIG. 8: Flow of the anomalous exponents when approaching the roughening transition from the massive phase. Left: $\tilde{\lambda}_{\Lambda_0} = 6.43$, Right: $\tilde{\lambda}_{\Lambda_0} = 6.442946808$. The closer the noise vertex is tuned to the critical value, the longer for the scaling plateau at which $\zeta_{d^K} = \zeta_\gamma = 0.54$ for $d = 3$ from Eq. (8). The flow goes from the UV (left of plot) to IR (right of plot) via $\Lambda = \Lambda_0 \exp(-s)$. At some point the scaling stops, both anomalous exponents become zero, because we are still in the massive phase.

value of the rescaled noise vertex $\tilde{\lambda}_{\Lambda_0}$ is varied to obtain the phase diagram Fig. 1. The condition for the phase boundary is the vanishing of the physical mass in the infrared $\Delta_{\Lambda \rightarrow 0} \rightarrow 0$.

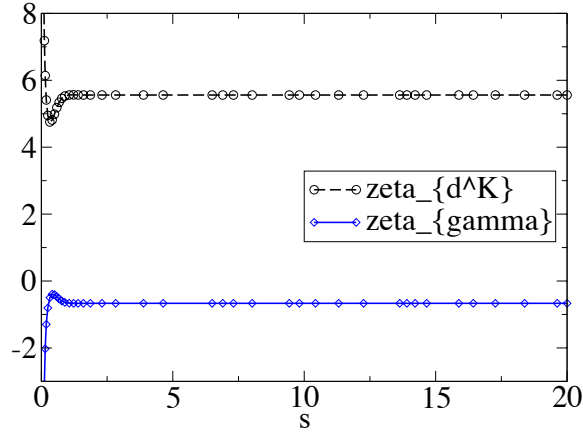


FIG. 9: Flows deep in the rough phase in which no remnant of the roughening transition (as in Fig. 2) is visible and the anomalous exponents very quickly attain their rough phase fixed point values $\zeta_{d^K} = 5.56$ and $\zeta_\gamma = -0.66$ from Table I in $d = 3$. Initial value of the noise vertex is $\tilde{\lambda}_{\Lambda_0} = 30 \gg \tilde{\lambda}_{\Lambda_0,c} = 6.4429468082319$. The flow goes from the UV (left of plot) to IR (right of plot) via $\Lambda = \Lambda_0 \exp(-s)$.

V. CONCLUSIONS

This paper pursued the strategy to (i) take an important universality class for non-equilibrium statistical mechanics (Burgers-Kardar-Parisi-Zhang equation), (ii) strip it from an important conservation law(s) (Galilean invariance), and (iii) compute the phase diagram and critical exponents using the dynamic renormalization group.

We broke the Galilean invariance by accounting for temporal correlations in the random driving force. The chief consequence of this is the absence of a fluctuation-dissipation relation in all spatial dimensions for sufficiently strong noise levels. We penetrated this strong noise “rough or turbulent” phase within a dynamic RG flow using frequency rescaling techniques that took care of long-time correlations in the noise. We computed exponents to one-loop order, essentially controlled close to four space dimensions $d = 4$. We showed that the rough phase is an example of self-organized criticality in the sense that its emergent gaplessness does not require fine tuning and traced this back to explicit cancellations in the one-loop β -functions. Higher loop analysis and numerical simulations will be needed to determine the fate of our theory beyond one-loop.

Sputtering an interface with correlations in time would be one physical example to which our results may apply. More intriguing are recent connections to quantum liquids and superfluids to KPZ scaling [11, 12] (in which more exotic types of noise can potentially be applied [34, 35]), and to waves in time-dependent random media [36, 37]. With regard to recent related works on nonlinear fluctuating hydrodynamics [38, 39], it will be interesting to systematically explore the role of broken conservation laws onto crossover time-scales in dynamics and transport [40].

Acknowledgments

We are indebted to Sebastian Diehl for discussions and help with the renormalization group truncation on the Keldysh contour. This work was supported by the DFG under grant Str 1176/1-1, by the Leibniz prize of A. Rosch, by the NSF under Grant DMR-1103860, by the Templeton foundation, by the Center for Ultracold Atoms (CUA), and by the Multidisciplinary University Research Initiative (MURI).

Appendix A: Threshold functions

We here tabulate the threshold functions appearing in the flow equations (38,39), $D_{\lambda^2}[\tilde{\Delta}]$, $S_{\lambda^2}[\tilde{\Delta}]$, and $G_{\lambda^3}[\tilde{\Delta}]$. We will give the pre-momentum integrated expression for general dimension d and the post-momentum integrated expression only for $d = 2$; the other dimensions do not qualitatively change their form.

The flow of the Keldysh component is determined by

$$S_{\lambda^2}^{(d)}[\tilde{\Delta}] = \int \frac{d^d \tilde{k}}{(2\pi)^d} \frac{2 \left((\tilde{\Delta} + \tilde{\mathbf{k}}^2)^2 + 3 \right)}{\left((\tilde{\Delta} + \tilde{\mathbf{k}}^2)^2 + 1 \right)^2} \Big|_{0 \leq \tilde{\mathbf{k}}^2 \leq 1}$$

$$\stackrel{d=2}{=} \frac{-2 \left(\tilde{\Delta}^2 + 1 \right) \left(\tilde{\Delta}(\tilde{\Delta} + 2) + 2 \right) \tan^{-1}(\tilde{\Delta}) + 2 \left(\tilde{\Delta}^2 + 1 \right) \left(\tilde{\Delta}(\tilde{\Delta} + 2) + 2 \right) \tan^{-1}(\tilde{\Delta} + 1) - \tilde{\Delta}(\tilde{\Delta} + 1) + 1}{2\pi \left(\tilde{\Delta}^2 + 1 \right) \left(\tilde{\Delta}(\tilde{\Delta} + 2) + 2 \right)} . \quad (\text{A1})$$

The flow of the mass variable is determined by

$$D_{\lambda^2}^{(d)}[\tilde{\Delta}] = \int \frac{d^d \tilde{k}}{(2\pi)^d} \frac{2 \left(\tilde{\Delta} + \tilde{\mathbf{k}}^2 \right) \left((\tilde{\Delta} + \tilde{\mathbf{k}}^2)^2 + 3 \right)}{\left((\tilde{\Delta} + \tilde{\mathbf{k}}^2)^2 + 1 \right)^2} \Big|_{0 \leq \tilde{\mathbf{k}}^2 \leq 1}$$

$$\stackrel{d=2}{=} \frac{\frac{4\tilde{\Delta}+2}{(\tilde{\Delta}^2+1)(\tilde{\Delta}(\tilde{\Delta}+2)+2)} + \log \left(\frac{2\tilde{\Delta}+1}{\tilde{\Delta}^2+1} + 1 \right)}{4\pi} . \quad (\text{A2})$$

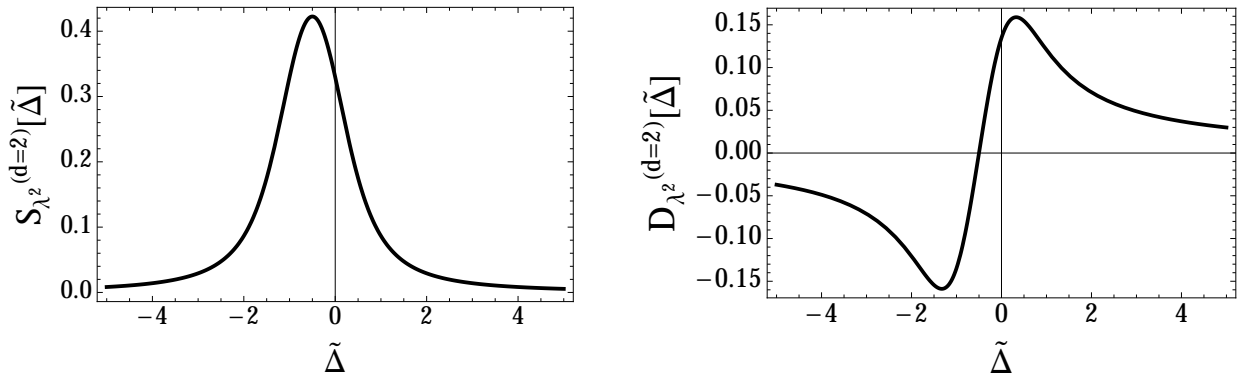


FIG. 10: Plots of the threshold functions for the Keldysh component (left) and the mass (right) in $d = 2$.

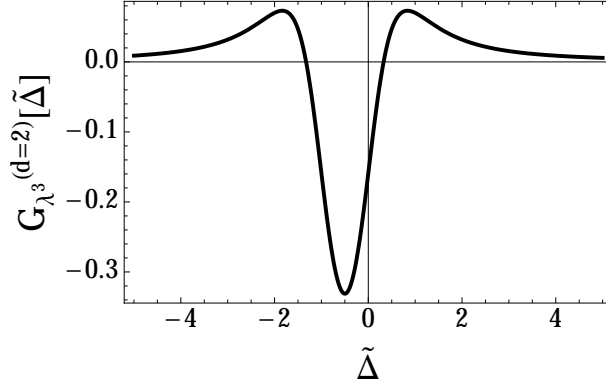


FIG. 11: Plot of the threshold functions for the noise vertex/frequency renormalization factor in $d = 2$.

The flow of the noise vertex (and the frequency renormalization factor) is determined by

$$\begin{aligned}
 G_{\lambda^3}^{(d)}[\tilde{\Delta}] &= \int \frac{d^d \tilde{k}}{(2\pi)^d} \frac{2 \left((\tilde{\Delta} + \tilde{k}^2)^2 ((\tilde{\Delta} + \tilde{k}^2)^2 + 6) - 3 \right)}{\left((\tilde{\Delta} + \tilde{k}^2)^2 + 1 \right)^3} \Big|_{0 \leq \tilde{k}^2 \leq 1} \\
 &\stackrel{d=2}{=} \frac{\tilde{\Delta}(\tilde{\Delta} + 1)(\tilde{\Delta}^2 + \tilde{\Delta} + 1)(\tilde{\Delta}^2 + \tilde{\Delta} + 6) - 4}{2\pi (\tilde{\Delta}^2 + 1)^2 (\tilde{\Delta}(\tilde{\Delta} + 2) + 2)^2}.
 \end{aligned} \tag{A3}$$

-
- [1] H. M. Jaeger, and A. J. Liu, *Far-From-Equilibrium Physics: An Overview*, [arXiv:1009.4874](https://arxiv.org/abs/1009.4874), Condensed Matter and Materials Physics: the science of the world around us, National Academies Press, Washington, DC (2007).
 - [2] S. Sotiriadis, and J. Cardy, *Quantum quench in interacting field theory: A self-consistent approximation*, Phys. Rev. B **81**, 134305 (2010).
 - [3] M. Kardar, G. Parisi, and Y.-C. Zhang, *Dynamic Scaling of Growing Interfaces*, Phys. Rev. Lett. **56**, 889 (1986).
 - [4] D. Forster, D. R. Nelson, and M. J. Stephen, *Large-distance and long-time properties of a randomly stirred fluid*, Phys. Rev. A **16**, 732 (1977).
 - [5] T. Nattermann, and L.-H Tang, *Kinetic surface roughening. I. The Kardar-Parisi-Zhang equation in the weak-coupling regime*, Phys. Rev. A **45**, 715 (1992).

- [6] J. P. Bouchaud, M. Mezard, and G. Parisi, *Scaling and intermittency in Burgers turbulence*, Phys. Rev. E **52**, 3656 (1995).
- [7] J. Berges, K. Boguslavski, S. Schlichting, and R. Venugopalan, *Basin of attraction for turbulent thermalization and the range of validity of classical-statistical simulations*, [arXiv:1312.5216](#) (2013).
- [8] S. Mathey, T. Gasenzer, and J. M. Pawłowski, *Anomalous scaling at non-thermal fixed points of Burgers' and Gross-Pitaevskii turbulence*, [arXiv:1405.7652](#) (2014).
- [9] V. Yakhot, and S. A. Orszag, *Renormalization-Group Analysis of Turbulence*, Phys. Rev. Lett. **57**, 1722 (1986).
- [10] V. Yakhot, and Z.-S. She, *Long-Time, Large-Scale Properties of the Random-Force-Driven Burgers Equation*, Phys. Rev. Lett. **60**, 1840 (1988).
- [11] M. Kulkarni, and A. Lamacraft, *Finite-temperature dynamical structure factor of the one-dimensional Bose gas: From the Gross-Pitaevskii to the Kardar-Parisi-Zhang universality class of dynamical critical phenomena*, Phys. Rev. A **88**, 021603 (R) (2013).
- [12] M. Arzamasovs, F. Bovo, and D. M. Gangardt, *Kinetics of Mobile Impurities and Correlation Functions in One-Dimensional Superfluids at Finite Temperature*, Phys. Rev. Lett. **112**, 170602 (2014).
- [13] E. Altman, *et al.*, *Two-dimensional superfluidity of exciton-polaritons requires strong anisotropy*, [arXiv:1311.0876](#) (2013).
- [14] G. Grinstein, M. A. Munoz, and Y. Tu, *Phase Structure of Systems with Multiplicative Noise*, Phys. Rev. Lett. **76**, 4376 (1996).
- [15] E. Medina, T. Hwa, M. Kardar, Y.-C. Zhang, *Burgers equation with correlated noise: Renormalization-group analysis and applications to directed polymers and interface growth*, Phys. Rev. A **39**, 3053 (1989).
- [16] P. Bak, C. Tang, and K. Wiesenfeld, *Self-Organized Criticality: An Explanation of $1/f$ Noise*, Phys. Rev. Lett. **59**, 381 (1987).
- [17] H. K. Janssen, U. C. Täuber, and E. Frey, *Exact results for the Kardar-Parisi-Zhang equation with spatially correlated noise*, Eur. Phys. J B **9**, 491 (1999).
- [18] J. Bonart, L. F. Cugliandolo, and A. Gambassi, *Critical Langevin dynamics of the $O(N)$ -Ginzburg-Landau model with correlated noise*, J. Stat. Mech. P01014 (2012).
- [19] E. Frey, and U. C. Täuber, *Two-loop renormalization-group analysis of the Burgers-Kardar-Parisi-Zhang equation*, Phys. Rev. E **50**, 1024 (1994).
- [20] T. Hwa, and M. Kardar, *Dissipative Transport in Open Systems: An Investigation of Self-Organized*

- Criticality*, Phys. Rev. Lett. **62**, 1813 (1989).
- [21] G. Grinstein, D.-H. Lee, and S. Sachdev, *Conservation laws, Anisotropy, and "Self-Organized Criticality" in Noisy Nonequilibrium Systems*, Phys. Rev. Lett. **64**, 1927 (1990).
 - [22] A. Kamenev, *Field Theory of Non-Equilibrium Systems*, Cambridge University Press, Cambridge (2011).
 - [23] E. G. Dalla Torre, S. Diehl, M. D. Lukin, S. Sachdev, and P. Strack, *Keldysh approach for nonequilibrium phase transitions in quantum optics: Beyond the Dicke model in optical cavities*, Phys. Rev. A **87**, 023831 (2013).
 - [24] D. A. Huse, C. L. Henley, and D. S. Fisher, *Huse, Henley, and Fisher Respond*, Phys. Rev. Lett. **55**, 2924 (1985).
 - [25] U. Dekker and F. Haake, *Fluctuation-dissipation theorems for classical processes*, Phys. Rev. A **11**, 2043 (1975).
 - [26] R. Gezzi, T. Pruschke, and V. Meden, *Functional renormalization group for nonequilibrium quantum many-body systems*, Phys. Rev. B **75**, 045324 (2007).
 - [27] L. M. Sieberer, S. D. Huber, E. Altman, and S. Diehl, *Non-equilibrium Functional Renormalization for Driven-Dissipative Bose-Einstein Condensation*, Phys. Rev. B **89**, 134310 (2014).
 - [28] P. Strack, R. Gersch, and W. Metzner, *Renormalization group flows for fermionic superfluids at zero temperature*, Phys. Rev. B **78**, 014522 (2008).
 - [29] K.-U. Giering, and M. Salmhofer, *Self-energy flows in the two-dimensional repulsive Hubbard model*, Phys. Rev. B **86**, 245122 (2012).
 - [30] A. M. Polyakov, *Gauge fields and Strings*, CRC Press (Chur) (1987).
 - [31] Y. Huh, P. Strack, and S. Sachdev, *Conserved current correlators of conformal field theories, in 2 + 1 dimensions*, Phys. Rev. B **88**, 155109 (2013).
 - [32] W. Metzner, M. Salmhofer, C. Honerkamp, V. Meden, and K. Schoenhammer, *Functional renormalization group approach to correlated fermion systems*, Rev. Mod Phys. **84**, 299 (2012).
 - [33] K. G. Wilson and M. E. Fisher, *Critical Exponents in 3.99 Dimensions*, Phys. Rev. Lett. **28**, 240 (1971).
 - [34] E. G. Dalla Torre, E. Demler, T. Giamarchi, and E. Altman, *Dynamics and universality in noise-driven dissipative systems*, Phys. Rev. B **85**, 184302 (2012).
 - [35] M. Buchhold, and S. Diehl, *Non-Equilibrium Universality in the Heating Dynamics of Interacting Luttinger Liquids*, [arXiv:1404.3740](https://arxiv.org/abs/1404.3740) (2014).

- [36] L. Levi, Y. Krivolapov, S. Fishman, and M. Segev, *Hyper-transport of light and stochastic acceleration by evolving disorder*, Nature Physics **8**, 912 (2012).
- [37] L. Saul, M. Kardar, and N. Read, *Directed waves in random media*, Phys. Rev. A **45**, 8859 (1992).
- [38] H. v. Beijeren, *Exact Results of Anomalous Transport in One-Dimensional Hamiltonian Systems*, Phys. Rev. Lett. **108**, 180601 (2012).
- [39] C. B. Mendl, and H. Spohn, *Dynamic Correlators of Fermi-Pasta-Ulam Chains and Nonlinear Fluctuating Hydrodynamics*, Phys. Rev. Lett. **111**, 230601 (2013).
- [40] J. Lux, J. Müller, A. Mitra, and A. Rosch, *Hydrodynamic long-time tails after a quantum quench*, Phys. Rev. A **89**, 053608 (2014).